ACCOUNTS
of chemical research

Biological and Biomedical Applications of Two-Dimensional Vibrational Spectroscopy: Proteomics, Imaging, and Structural Analysis

FREDERIC FOURNIER,[†] RUI GUO,[†] ELIZABETH M. GARDNER,[†] PAUL M. DONALDSON,[†] CHRISTIAN LOEFFELD,[†] IAN R. GOULD,[†] KEITH R. WILLISON,[‡] AND DAVID R. KLUG*,[†]

[†]Department of Chemistry and Chemical Biology Centre, Imperial College London, Exhibition Road, London SW7 2AZ, U.K., [‡]Institute of Cancer Research, Chester Beatty Laboratories, Cancer Research U.K., Centre of Cellular and Molecular Biology, London SW3 6JB, U.K.

RECEIVED ON MARCH 10, 2009

CONSPECTUS

In the last 10 years, several forms of two-dimensional infrared (2DIR) spectroscopy have been developed, such as IR pump−probe spectroscopy and photon-echo techniques. In this Account, we describe a doubly vibrationally enhanced four-wave mixing method, in which a third-order nonlinear signal is generated from the interaction of two independently tunable IR beams and an electron-polarizing visible beam at 790 nm. When the IR beams are independently in resonance with coupled vibrational transitions, the signal is enhanced and cross-peaks appear in the spectrum. This method is known as either DOVE (doubly vibrationally enhanced) four-wave mixing or EVV (electron−vibration−vibration) 2DIR spectroscopy.

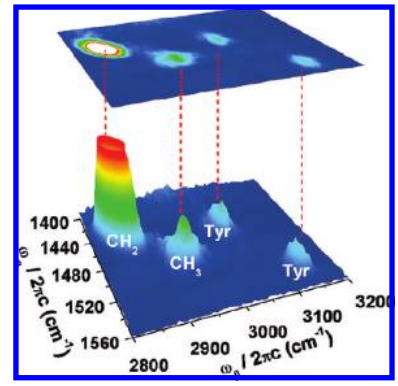

We begin by discussing the basis and properties of EVV 2DIR. We then discuss several biological and potential biomedical applications. These include protein identification and quantification, as well as the potential of this label-free spectroscopy for protein and peptide structural analysis. In proteomics, we also show how post-translational modifications in peptides (tyrosine phosphorylation) can be detected by EVV 2DIR spectroscopy.

The feasibility of EVV 2DIR spectroscopy for tissue imaging is also evaluated. Preliminary results were obtained on a mouse kidney histological section that was stained with hematoxylin (a small organic molecule). We obtained images by setting the IR frequencies to a specific cross-peak (the strongest for hematoxylin was obtained from its analysis in isolation; a general CH_3 cross-peak for proteins was also used) and then spatially mapping as a function of the beam position relative to the sample. Protein and hematoxylin distribution in the tissue were measured and show differential contrast, which can be entirely explained by the different tissue structures and their functions.

The possibility of triply resonant EVV 2DIR spectroscopy was investigated on the retinal chromophore at the centre of the photosynthetic protein bacteriorhodopsin (bR). By putting the visible third beam in resonance with an electronic transition, we were able to enhance the signal and increase the sensitivity of the method by several orders of magnitude. This increase in sensitivity is of great importance for biological applications, in which the number of proteins, metabolites, or drug molecules to be detected is low (typically pico- to femtomoles). Finally, we present theoretical investigations for using EVV 2DIR spectroscopy as a structural analysis tool for inter- and intramolecular interaction geometries.

1. Introduction

There are a number of forms of coherent multidimensional spectroscopy that have emerged as useful tools in a variety of research contexts. Each of these methods has particular strengths and capabilities that make them more or less suitable for addressing particular scientific questions. We have been exploring the utility of one family of 2DIR methods for a range of biological and bio-

Published on the Web 06/23/2009 www.pubs.acs.org/acr
10.1021/ar900074p CCC: $71.50

medical applications. The approach, originally demonstrated by John Wright and colleagues,[1−6] is known as electronic−vibration−vibration two-dimensional infrared spectroscopy (EVV 2DIR) or as DOVE-IR (doubly-vibrationally enhanced infrared spectroscopy). The purpose of this Account is to give a broad overview of what is currently possible and indicate what might realistically become possible, using this particular form of 2DIR with respect to biological and biomedical applications. It is entirely possible that other forms of spectroscopy including other forms of 2DIR may be able to do as well or better than EVV 2DIR with respect to some of these applications. But in this Account, we restrict ourselves to discussing this one class of methods.

2. The Basis of EVV 2DIR

EVV 2DIR has some significantly different properties compared with other published forms of 2DIR spectroscopy. This leads to particular strengths and weaknesses and also has implications for the practical implementation of EVV 2DIR experiments. This section is intended to highlight those qualities that differ from other methods.

2.1. The Practicalities of EVV 2DIR Experiments. In EVV 2DIR, three independently tunable and independently timed picosecond pulsed laser beams are brought together on a sample in a phase-matched configuration. Two of these beams are in the infrared and are used to excite molecular vibrations, while the third is a visible beam and is essentially used to probe the polarization generated by the two IR beams, such that the coupling strength of the two vibrations can be "read-out" by the detection of visible photons. The signal is detected at the frequency $\omega_\delta = \omega_\gamma + \omega_\beta - \omega_\alpha$ (with ω_α and ω_β representing the IR frequencies and ω_γ the visible beam frequency). The final "read-out" step is essentially half of a conventional Raman scattering event, but coherent. One of the consequences of this is that the electronic properties of the molecular system also affect the signal and that the experiment can be made triply resonant if the visible "probe" beam is tuned toward an electronic resonance.

The IR beams are independently scanned in frequency and when they are in resonance with coupled vibrational modes the detected signal is multiplicatively enhanced. The spectra represent the level of signal detected at ω_γ as a function of the IR frequencies; they show cross-peaks at the specific IR frequencies corresponding to coupled vibrational modes. Two delay stages control the timing between the pulses: when not further discussed, T_{12} and T_{23} denote the delay of the IR pulse at ω_β relative to ω_α and of the 800 nm pulse relative to the IR at ω_β, respectively.

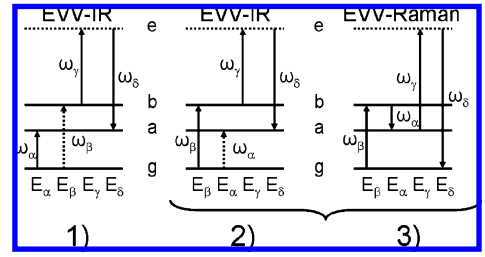

FIGURE 1. Wave-mixing energy-level diagrams depicting the four-wave-mixing EVV processes. $\mathbf{E}_\alpha$ and $\mathbf{E}_\beta$ are the accordable infrared electric fields, $\mathbf{E}_\gamma$ is the visible incident electric field, and $\mathbf{E}_\delta$ is the detected four-wave-mixing (FWM) EVV electric field. When $\mathbf{E}_\alpha$ and $\mathbf{E}_\beta$ are resonant with coupled vibrational modes (levels a and b, respectively) the FWM EVV signal is multiplicatively enhanced (whence the original name for the technique of DOVE four-wave mixing). The pathway 1 is for $\mathbf{E}_\alpha$ arriving first on the sample; the pathways 2 and 3 are for $\mathbf{E}_\beta$ arriving first.

2.2. Properties of EVV 2DIR. One of the most obvious and unusual aspects of EVV 2DIR is that it involves not only the excitation of molecular vibrations with infrared laser pulses but also the direct polarization of electrons via a "half-Raman" scattering step. This makes EVV 2DIR effectively a hybrid Raman−IR method where the final signal strength depends on both IR and Raman processes. This is perhaps most clearly demonstrated when EVV 2DIR spectra are calculated from first principles.[3,7]

Another important property is that all of the EVV 2DIR experiments performed to date have involved direct excitation of vibrational combination bands, usually in the near-infrared. Vibrational combination bands are created by the anharmonic coupling of two vibrational modes. In general, two types of anharmonicities will contribute: mechanical anharmonicity, which measures the deviation of the molecular potential energy surface from simple harmonic potential, and electrical anharmonicity, which is the nonlinearity of the molecular dipole moment along vibrational coordinates.[8] This means that EVV 2DIR is sensitive to couplings that arise from purely mechanical anharmonicity, from purely electrical anharmonicity, or from both. The processes that contribute to the total EVV signal are shown in Figure 1.

It can be seen that pathway 3 is essentially the same as coherent anti-Stokes Raman spectroscopy (CARS), but with the involvement of real excited states rather than the purely virtual states of a CARS experiment. Pathways 2 and 3 are only accessible if the near-infrared pulse that excites the combination band comes first. Thus it is possible to switch pathways on and off by changing the pulse ordering, and this additional

flexibility conveys some additional utility to the EVV method as discussed below.

2.3. Breaking the Fixed Fourier Relationship in 2DIR: Enhanced Decongestion of 2DIR Spectra. The independent timing of the infrared and visible pulses has an important consequence, namely, that it is possible to break the fixed transform relationship between wavelength and time that is used in the current pump−probe or echo variants of 2DIR. This means that pathways that are always present in other forms of 2DIR can be switched off in EVV 2DIR by manipulation of the pulse timings. This is seen clearly in the situation where Fermi resonances are present as in the case of benzene.[7] EVV 2DIR has the advantage of offering enhanced spectral decongestion with other parameters such as delays between pulses and beam polarizations providing yet additional control of spectral congestion.[9,10]

2.4. Sensitivity to Pure Electrical Anharmonicity. One of the more unusual properties of EVV 2DIR is that it is not a difference spectroscopy. As a consequence of this, cross-coupling can be observed even in the case where the mechanical anharmonicity is either too small to shift ground and excited vibrational states significantly or entirely absent.[7,9] The corollary of this is that the other 2DIR techniques demonstrated to date are not able to measure couplings that are purely electrical unless the electrical coupling is sufficiently strong to cause secondary mechanical anharmonicity.

A good example of such a case is the methyl and methylene stretch or deformation overtone, coupled with the scissor deformation mode. Both methyl and methylene features appear as strong and highly reproducible features in EVV 2DIR spectra of peptides and proteins, and we have studied them extensively. Calculations suggest that these modes have either very weak or zero mechanical anharmonic coupling but significant electrical anharmonicity.[9]

In order to demonstrate that these features are indeed the result of pure electrical anharmonicity, we use the independent pulse timings available in EVV 2DIR to extinguish the signal via interference of pathways 2 and 3 (Figure 1). If the time ordering of the IR pulses is reversed ($\mathbf{E}_\beta$ first) from the timing usually used ($\mathbf{E}_\alpha$ first), then pathway 1 no longer contributes, and the signal is the sum of the contributions of pathways 2 and 3. Pathways 2 and 3 have opposite sign, and therefore if the combination band is unshifted by the interaction of modes a and b, as is the case when there is zero mechanical anharmonicity, then the signals will totally cancel. The spectra shown in Figure 2 demonstrate this effect: when only pathway 1 is opened ($\mathbf{E}_\alpha$ first), CH_2 and CH_3 cross-peaks are present in the spectrum, whereas when the IR pulses order is reversed ($\mathbf{E}_\beta$ first), these two cross-peaks disappear. If there is a level shift, then splitting of the cross-peaks is observed as pathways 2 and 3 are no longer degenerate.[7]

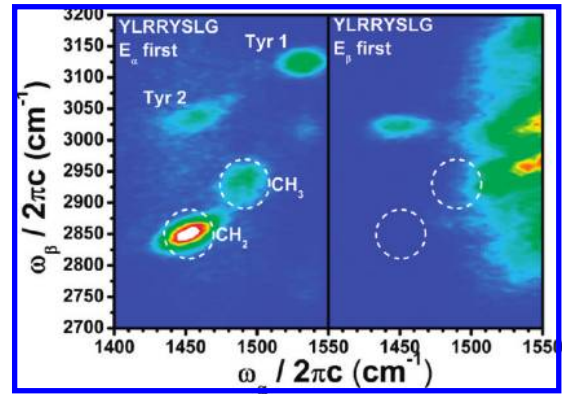

FIGURE 2. EVV 2DIR spectra of a short peptide (YLRRYSLG) measured for two pulse orderings demonstrating the cancellation of pathways 2 and 3 and that therefore the methyl and methylene peaks result from pure electric anharmonic coupling. $\mathbf{E}_\alpha$ pulse first, left side spectrum; $\mathbf{E}_\beta$ pulse first, right side spectrum. The spectra are measured with the same relative delay differences of 1 ps ($T_{12} = 1$ ps, $T_{23} = 1$ ps) and are represented with the same intensity scale.

The cancellation of pathways 2 and 3 in the case of pure electrical anharmonicity (absence of mechanical anharmonicity) appears to be more or less total with less than 3% of the signal remaining for the CH_2 cross-peak.

3. Biological and Biomedical Applications of EVV 2DIR

3.1. Proteomics. The field of proteomics is the identification and characterization of proteins on a large scale and at high throughput to provide data for the discovery and analysis of protein networks and to obtain a global view of cellular processes at the protein level, the so-called "proteome".[11−13] The proteome describes the number of each protein in a specific cell, the interactions of the proteins, and post-translational modifications of the proteins and allows one in principle to monitor any changes in the cellular pathways due to disease, drug action, or other biological perturbations. Determination of a proteome is an intensive task requiring protein identification, quantification, and analysis of post-translational modification and protein complexation. In so-called "bottom-up" proteomics, the proteins to be identified are digested by an enzymatic or chemical process and the resulting peptides analyzed, usually by mass spectrometry. In the second approach, the "top-down" strategy, the intact protein system is studied. The bottom-up approach is widely used and commercial instruments exploiting this strategy are available. Top-down approaches have the advantage of requiring no

additional chemical−biochemical preparative steps associated with producing fragments and, as the bottom-up approach, allowing the study of native proteins and native protein properties.

We are in the process of developing EVV 2DIR spectroscopy as an analysis tool for proteomics. The initial goal is to be able to identify proteins and in the future analyze the identified proteins in greater detail, such as assessing the extent and type of their post-translational modifications. Our protein identification strategy is based on using EVV 2DIR to quantify the amino acid content of a protein. EVV 2DIR is shown to be able to perform absolute quantification, something of major importance in the field of proteomics but rather difficult and time-consuming to achieve with mass spectrometry. Our technique can be qualified as a top-down label-free method; it does not require intensive sample preparation, the proteins are intact when analyzed, and it does not have any mass restriction on the proteins to be analyzed. Moreover, EVV 2DIR is a nondestructive technique; the samples can be kept for reanalysis in the light of further information.

3.1.1. Identifying and Counting Proteins. Known small peptides were used to identify tyrosine, phenylalanine, and CH_2 specific vibrational signatures in the EVV 2DIR spectra. We showed that the square root of the relative intensity of the cross-peaks is proportional to the amount of amino acid relative to the CH_2 internal reference cross peak.[14] When applied to a set of 10 known proteins, these same amino acid signatures are detected, as well as a tryptophan cross-peak and a CH_3 feature used as internal reference (Figure 3).

Figure 4 shows that there is indeed a direct correlation between the EVV 2DIR features signal level for each amino acid and the known amount of that amino acid in ten test proteins. This direct proportionality suggests that these cross-peaks are not structurally sensitive and that this approach can be applied efficiently to protein identification.

The curves of relative amino acid quantification (Figure 4) are the starting point of a protein differentiation procedure based on probability of identicality.[10] Briefly, each amino acid/CH_3 ratio is described by a normal distribution with a width determined by the standard deviation of the data shown in Figure 4. The fingerprint of one protein is defined as a product of *N* orthogonal normal distributions corresponding to *N* amino acid number ratios, *N* being the number of identified amino acid cross peaks or the number of amino acids used for the differentiation strategy. The comparison of two proteins is performed by calculating the overlap integrals of their numerical fingerprint: if the distributions are exactly overlapped, the integral is maximum and the proteins are indistinguishable;

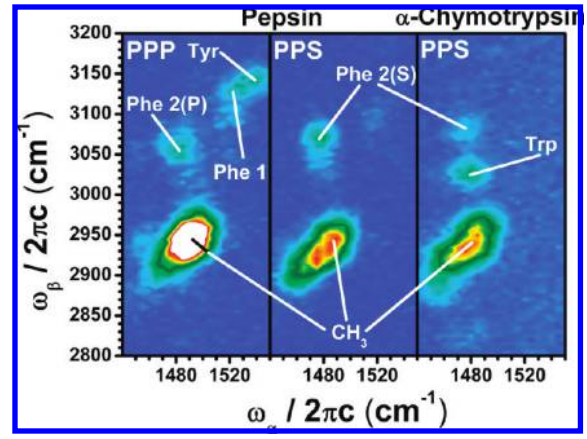

FIGURE 3. Examples of typical EVV 2DIR spectra of two proteins: pepsin and a tryptophan-rich protein, α-chymotrypsin. To illustrate the effect of the visible beam polarization, two different polarization combinations are shown for the pepsin spectrum: PPP (all beams having their fields in the plane of propagation) and PPS (IR beams polarized in the plane of propagation and the visible normal to the IRs). The spectra are measured for the same set of pulse delays (T_{12} = 2 ps; T_{23} = 1 ps) and plotted with different intensity scale. Significant amino acid and CH_3 internal reference cross peaks are labeled.

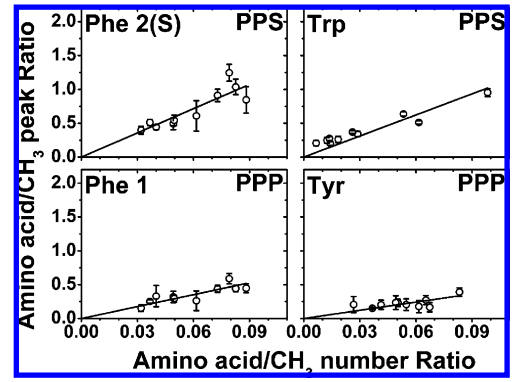

FIGURE 4. Measured ratios of amino acid peak intensity to internal reference intensity plotted against the known ratios for the four identified amino acid peaks (PPP and PPS note the beam polarization configuration). Each data point comes from one of the ten proteins. The solid lines are the linear fits constrained through the origin.

on the contrary, if the distributions are totally different, the integral is zero and the proteins are totally distinguishable. These overlap integrals, when normalized to the value obtained from comparing one protein with itself, define a probability of identicality of two proteins. Protein differentiation maps represent the probability of identicality as a two-dimensional graph where the gray level of each square reflects the probability of two proteins to be identical (Figure 5).

Bioinformatics studies suggest that identifying the relative levels of only five amino acids with 15% precision would allow 44% of the proteins in the ENSEMBL human protein

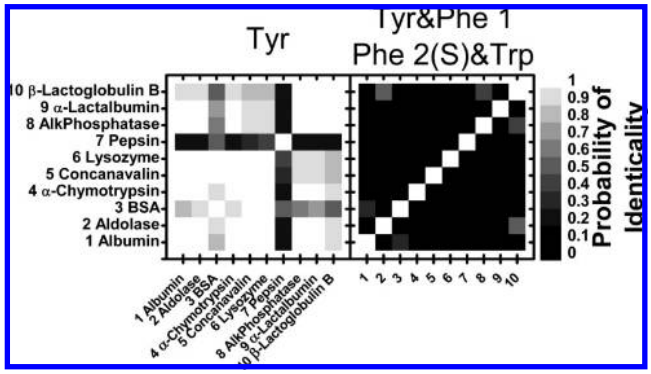

FIGURE 5. Differentiation maps of the ten proteins studied using the tyrosine peak only and the full set of amino acid peaks (Tyr, Phe1, Phe2(S) and Trp cross peaks as noted in Figure 3). White squares correspond to normalized overlap integral values of 1 (completely indistinguishable) and black to 0 (completely distinguishable). The gray level of each square reflects the probability that the two proteins being compared are the same protein. The diagonal compares a protein with itself and so is white. The relative darkness of an entire map shows the relative contribution of each amino acid scheme in distinguishing the proteins.

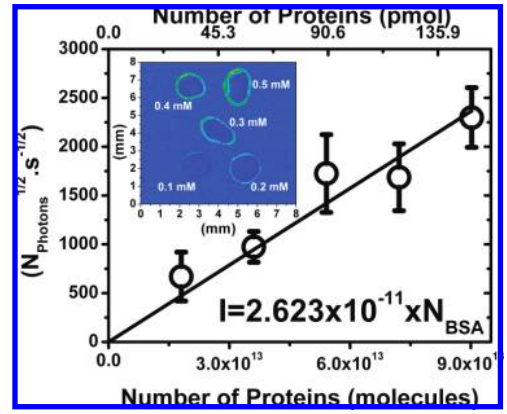

FIGURE 6. Square root of the EVV 2DIR signal level as a function of the number of protein molecules in the sample. The signal level of the CH_3 peak at 1485/2930 was mapped across five deposited films (drop volume, 0.3 μL) of BSA at five different concentrations (0.5, 0.4, 0.3, 0.2, and 0.1 mM; EVV 2DIR image of the deposits are shown in the inset, 1 s acquisition time per pixel with delays set at $T_{12} = 1.5$ ps and $T_{23} = 1$ ps and 70 μm step size). The integrated EVV 2DIR intensity (I) of the square-rooted image for each dried drop is plotted against the total number of protein molecules (N_{BSA}) in the corresponding drop. The error bars are standard deviations from four repeats performed on four different sets of five protein samples. The solid lines represent the linear fit; the equation for the fit is also shown. Note that the images have a bright ring around the edge of each spot due to the "coffee-ring effect" which causes the protein to dry at highest concentrations on the periphery of each droplet.

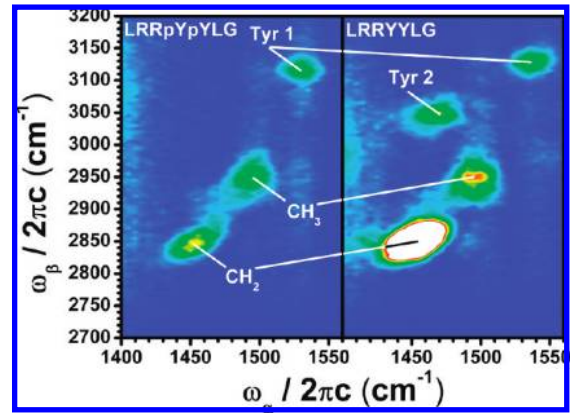

FIGURE 7. EVV 2DIR spectra of two versions of the same peptide: the tyrosine phosphorylated (labeled "pY" in the amino acid sequence) and nonphoshorylated version. The spectra are recorded for the same set of delays ($T_{12} = 1.5$ ps and $T_{23} = 1$ ps) and for all the beams polarized P. The spectra are plotted with the same intensity scale.

database (~33 000 proteins)[15] to be uniquely identified and 72% to be one of only two proteins; 60% would be unambiguously identified if the molecular weight of the proteins is used as a parameter as well.

The speed of this process is high enough to consider EVV 2DIR as a real proteomics tool, because each amino acid peak can be quantified to sufficient precision with around 10−60 s of signal averaging giving around 1−4 min per protein depending on the search pattern used.

Finally there is the issue of absolute quantification. Because of spatial heterogeneity of the protein sample (a dried drop of protein solution placed on a substrate), it is better to map the signal across the whole sample than to compare the CH_3 cross peak intensity on local spots on each dried film. It is then possible to determine the total integrated intensity and check for linearity (Figure 6).

3.1.2. Post-translational Modifications. The phosphorylation of amino acids is of major importance in regulating protein activity. To see whether we could identify phosphorylation of tyrosine, we made identical peptides containing two tyrosines and two phosphorylated tyrosines. These were diluted in water at the same concentrations and deposited on a stainless steel substrate. EVV 2DIR spectra were then measured in reflection (Figure 7).

The nonphosphorylated peptide (labeled LRRYYLG) shows the usual pattern consisting of CH_2 and CH_3 cross peaks and two aromatic cross peaks of tyrosine previously identify in our peptides studies (Tyr 1 and Tyr 2).[14] For the phosphorylated peptide (labeled LRRpYpYLG) the $(\delta CH_2,\nu_{13})/[(\delta CH_2,\nu_{13}) + (\delta CH_2,\nu_{16})]$ cross peak (Tyr 2) totally disappears whereas the $\nu_{13}/(\nu_{13} + \nu_{16})$ cross peak (Tyr 1) is red-shifted by ~12 cm^{-1} in the ω_β direction and ~6 cm^{-1} in the ω_α direction.

These preliminary results suggest that the intensity of the Tyr 2 cross peak is inversely proportional to the amount of phosphorylated tyrosines present in the peptide.

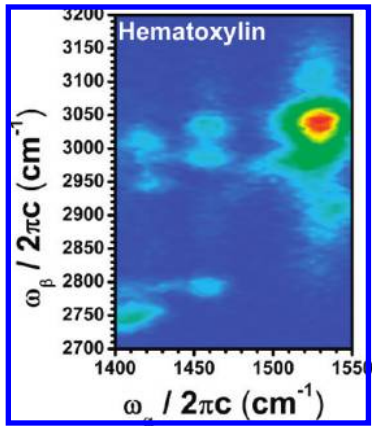

FIGURE 8. Hematoxylin EVV 2DIR spectrum measured at $T_{12} = 1$ ps and $T_{23} = 1$ ps.

3.2. Imaging. Optical imaging of cells or tissue samples is an important area in the life sciences. Chemically sensitive label-free imaging methods are particularly attractive in principle, and a range of approaches have been developed including IR, Raman, and CARS imaging. In all of these cases, chemical sensitivity is possible but due to the extensive congestion of the vibrational spectra in these samples, this is usually restricted to classes of molecules, such as proteins, fats, and nucleic acids, or to particular molecules present at very high concentration. EVV 2DIR spectroscopy has the potential to provide enhanced contrast in imaging of tissue samples by decongesting the spectra to a much greater extent than is possible with imaging methods based on techniques that use one spectral dimension. EVV 2DIR imaging could therefore be useful for providing alternative information on the spatial distribution of particular chemical species. We therefore show here a simple pilot experiment that demonstrates that EVV 2DIR can be used in such a manner.

To perform the tissue imaging, the IR frequencies are set on a cross-peak specific to a chemical group, the sample is spatially scanned and the signal level, detected by transmission, is mapped as a function of the beam position on the sample.

The validation experiments shown here are performed on histological sections of mouse kidney stained with hematoxylin. The ~5 μm thick tissue sections are deposited on 1.5 mm thick microscope glass slides. The purpose is to show that the distributions of hematoxylin can be determined within different tissue types of the kidney section by using a vibrational cross-peak as the contrast-providing feature.

Prior to the sample imaging, hematoxylin solution was deposited and allowed to dry on a microscope glass slide in order to measure its EVV 2DIR signatures (Figure 8).

The hematoxylin signal at the strongest cross peak (1530/3040 in Figure 8) was easily detected in the kidney section. From previous studies,[10] we know that EVV 2DIR spectra of proteins show a CH_3 cross peak at around 1490/2940, and this signal level was mapped as well.

Images were acquired for the two pairs of IR frequencies corresponding to the hematoxylin and the protein CH_3 (Figure 9).

The hematoxylin image reflects the distribution of cell nuclei and also ribonucleic acids since it stains mainly those entities. Differential contrast is clearly seen between the hematoxylin and the protein CH_3 images.

A simple histological interpretation of the kidney section is presented in Figure 10; a general anatomical description of the kidney structure can be found elsewhere.[16]

Hematoxylin stains nuclei and also ribonucleic acids necessary for protein synthesis. High levels of hematoxylin are measured in the cortical and medulla areas and a more dispersed signal in the collecting area. This is consistent with the presence of cells with nuclei in these areas. Instead, the blood clot contains cells without nuclei (red blood cells and platelets), which do not fix hematoxylin, hence the lack of signal.

Hemoglobin and fibrin present in large amounts in the blood clot give rise to a strong protein signal. Protein signal is high as well in the cortical area where cells are involved in urine formation and thus contain energetic machinery and synthesize a large amount of proteins. Weaker signals are measured in the medulla and collecting areas where cells are mainly involved in exchange of water and ions and structure and transport, respectively.

3.3. Enzyme Mechanisms. One field in which time-resolved spectroscopy has a significant impact is the study of enzyme mechanisms. This has largely been restricted to reactions that are naturally light-triggered, such as photosynthetic or visual processes, but has also included cases of direct photolysis[17−19] and the release of caged compounds by photolysis.[20]

Mechanistic studies have up to now used one-dimensional spectroscopy to study the formation of intermediate states during enzyme-catalyzed reactions, but in principle the information content of a multidimensional spectroscopy should be greater. In this section, we demonstrate the use of electronically resonant EVV 2DIR to selectively observe structural elements of a particular protein's active site, namely the retinal chromophore at the center of the photosynthetic protein bacteriorhodopsin (bR), while avoiding signal from the surrounding protein. By tuning the visible beam close to resonance with an electronic transition during an EVV 2DIR experiment, one should get considerable enhancement of the signal size in the same way as occurs with resonance Raman scattering.

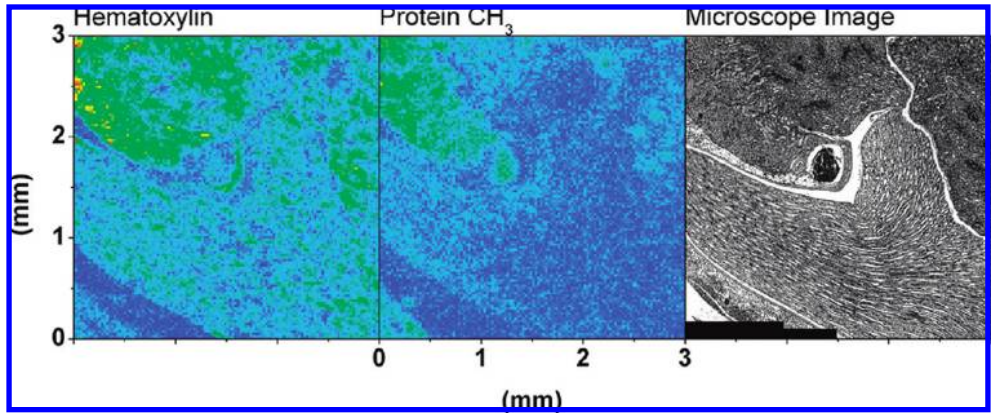

FIGURE 9. EVV 2DIR images and a visible microscope image of the kidney section area investigated. For EVV 2DIR, the signal is mapped across the sample for $T_{12} = 1$ ps and $T_{23} = 1$ ps for two pairs of IR frequencies corresponding to the hematoxylin and the protein CH_3 cross peaks. The EVV 2DIR images are recorded point per point (1 s acquisition per point) with 25 μm step size. The sample is scanned horizontally in the same direction for every vertical position to create the 3 mm $\times$ 3 mm field. The level of EVV 2DIR signal increases from blue to green and red; both EVV 2DIR images are shown with the same intensity scale. The microscope image is made out of ten narrow field images stitched together to represent the area scanned by EVV 2DIR.

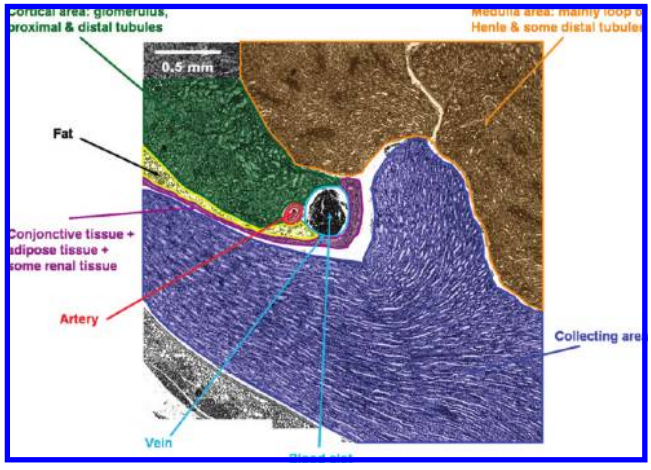

FIGURE 10. Interpretation of the kidney histological section showing the different kinds of tissue present in the area scanned by EVV 2DIR.

Triply resonant signal from bacteriorhodopsin membranes (isolated from *Halobacterium salinarium*) was observed at 1545/3050 cm^{-1} (inset of Figure 11b). The assignments of the coupled vibrational states giving rise to this cross peak were confirmed by DFT calculations. The modes being probed by the infrared pulses are a C═C stretch of the retinal's conjugated backbone, ν(C═C) (1545 cm^{-1}), and its first overtone, 2ν(C═C), (3050 cm^{-1}).

Numerous infrared and Raman studies have used the shifting in frequency of this C═C stretch for observing the intermediates of bacteriorhodopsin's photocycle.[21−23] Because the experiments here were carried out on samples at <1% humidity, the observed cross peak is attributable to various photoaccumulated and trapped intermediates of bR's dark-adapted photocycle (λ_{max} of the sample measured at 562 nm).[24,25]

An example of the level of signal enhancement possible using this triply resonant technique can be seen by comparison of the signal level from the methyl group of a protein with that from bacteriorhodopsin's retinal. At the end of section 3.1.1, we demonstrated how absolute quantification of proteins can be achieved with EVV 2DIR by imaging a sample on the protein CH_3 cross peak at 1485/2930 cm^{-1}. Here we show that the same quantification procedure can be performed for bacteriorhodopsin using the retinal feature at 1545/3050 cm^{-1}. To this end, a series of bacteriorhodopsin samples of varying concentrations is imaged on the retinal cross peak. Figure 11 compares calibration curves obtained for concanavalin A (chosen for its similar size to bR) imaged at 1485/2930 cm^{-1}, and for bacteriorhodopsin imaged on the 1545/3050 cm^{-1} retinal cross peak.

From the concanavalin A measurements, a sensitivity limit of 9×10^{12} protein molecules (~15 pmol) in the lasers interaction area was established. The bacteriorhodopsin measurements, however, give a sensitivity limit of 6×10^{10} molecules (0.1 pmol) in the laser interaction area. Considering an interaction area with a diameter of 80 μm and a probed sample thickness of 10 μm, these sensitivity limits would correspond to solutions of 0.3 mol/L for concanavalin A and 0.002 mol/L for bR. In terms of numbers of molecules therefore, the limit of detection it is possible to achieve for bR when probing its chromophore is 100 times lower than that for a protein when measuring its CH_3 cross peak. Moreover, considering that each concanavalin A molecule contains 139 CH_3 groups and that each bacteriorhodopsin molecule contains only one retinal chromophore, the CH_3 group and retinal detection limits in terms of number of chemical moieties are 1×10^{15} and $6 \times$

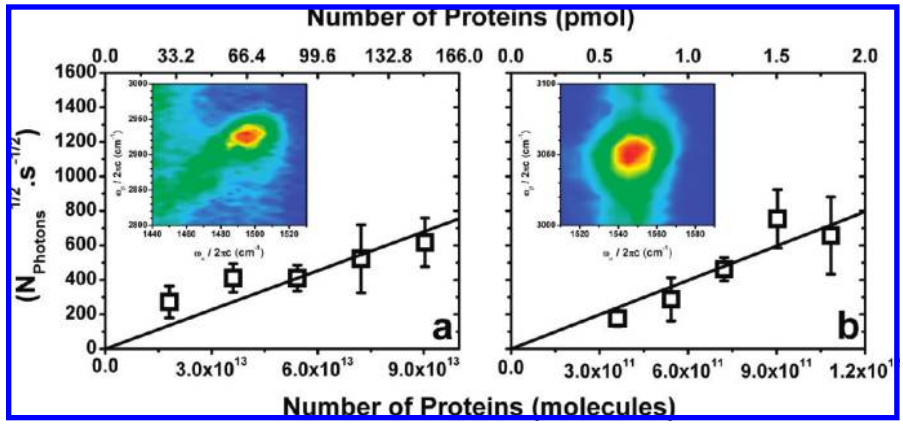

FIGURE 11. Square root of the EVV 2DIR signal level as a function of the number of concanavalin A (a) or bacteriorhodopsin (b) molecules in the sample. Insets of panels a and b are EVV 2DIR spectra showing the protein CH_3 and the retinal ν(C═C) cross peaks, respectively. For concanavalin A, the signal level of the CH_3 peak at 1485/2930 was mapped across five deposited films with concentrations of 0.1, 0.2, 0.3, 0.4, and 0.5 mM and a drop volume of 0.3 μL. For bacteriorhodopsin, the signal level of the retinal peak at 1545/3050 was mapped across films with concentrations of 2, 3, 4, 5, and 6 μM and a drop volume of 0.3 μL. For both concanavalin A and bacteriorhodopsin, the measurements were taken in reflection with delays of $T_{12} = 1$ ps and $T_{23} = 1$ ps, a 1 s acquisition time per pixel and a 100 μm step size. The integrated EVV 2DIR intensity of the square-rooted image for each dried drop is plotted against the total number of protein molecules (NConA or NbR). The error bars are standard deviations from four repeats performed on four different sets of five protein samples. The solid lines represent the linear fits.

10^{10}, respectively. Thus by using triply resonant EVV 2DIR, it is possible to achieve 10^4 times higher signal from retinal's conjugated backbone than it is from a protein CH_3 group. Therefore significant improvement in EVV 2DIR can be achieved by making the electronically polarizing visible "read out" beam preresonant with the molecular systems being studied. Further enhancement could be achieved in this case by tuning the visible beam (currently at 790 nm) closer to the 560 nm absorption maximum of the bR.

3.4. Structural Analysis: Measuring Structural Parameters via Electrical Anharmonicity in the Absence of Mechanical Anharmonicity. There have been a number of studies regarding the use of 2DIR spectroscopy to decipher the structures of small peptides.[26−29] This is a particularly challenging problem and one that will require a good deal more effort to solve. There are however many other categories of molecular structural analysis of great importance in the biological and biomedical sciences. A particular class of these is the study of the geometry of interaction between biomolecules that do not form a covalent bond or the geometry of interaction of chemical groups within large biomolecules such as proteins, which are often the interactions that convey various forms of biological function. In this section, we focus on this class of interactions and note that although our primary interest is in biomolecular interactions, the approach outlined here could potentially be used in other contexts where molecular species of interest are juxtaposed.

As discussed in section 2.4, one of the unusual features of EVV 2DIR spectroscopy is that it is sensitive to pure electrical coupling between molecular vibrations, that is, pure electrical anharmonicity. Good examples of this are the cases of the CH_2 and CH_3 modes shown in Figure 2 in section 2.4. These cross-peaks arise from pure electrical anharmonicity, a conclusion supported by both QM calculation and experimental evidence of the total cancellation of these features when pathways 2 and 3 are enabled by appropriate pulse ordering.

One of the useful properties of pure electrical anharmonicity is that it obeys simple physical rules for the distance and angle dependence of the coupling. It is already known that intermolecular electrical couplings between two groups should be inversely proportional to the third power of their distance as first proposed by Okumura et al.[30] and Cho[31] and later confirmed in CO−HCl dimer by Hahn et al.[32] By a theoretical survey of a series of molecules with formulas such as $HC{\equiv}C{-}(CH_2)_n{-}C{\equiv}N$ ($n = 2-4$), we were able to confirm that this relationship also exists for intramolecular electrical coupling as shown in Figure 12 between C≡C and C≡N groups, which largely couple with each other electrically.

Apart from this sensitivity to distance, the relative orientations of the interacting groups are almost as crucial. This can be illustrated by a theoretical examination of EVV 2DIR spectra of two conformers of 4-cyano-1-butyne ($HC{\equiv}C{-}(CH_2)_2{-}C{\equiv}N$), the anti and gauche conformers. Theory predicts that only the anti conformer exhibits two distinctive coupling cross peaks between the C≡C and C≡N stretching modes and none for the gauche one (Figure 13).

Since the distance between CC and CN groups is shorter in the gauche conformer (3.8 Å compared with 4.9 Å), this

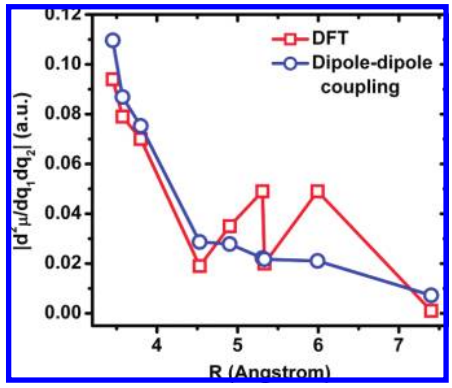

FIGURE 12. Relationship between the interaction distance *R* and the magnitude of electrical anharmonicity calculated at DFT level (red) and with a dipole−dipole coupling model (blue).

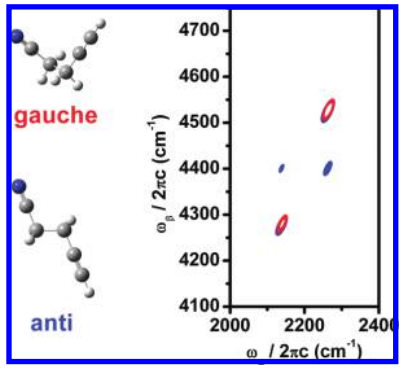

FIGURE 13. Calculated EVV 2DIR spectra of anti (blue) and gauche (red) conformers of 4-cyano-1-butyne at B3LYP/6-31+G(d,p) level.

should have given a greater signal by generating an electrical anharmonicity larger in magnitude. However the relative orientation of the two interacting groups in the gauche conformer means its resultant electrical anharmonicity lies at an angle from the directions of transition dipoles and transition polarizabilities of CC and CN groups, and this nonoptimal alignment makes the electrical anharmonicity unable to contribute to 2DIR signals. On the other hand, although the distance between the two groups is larger in the anti conformer, the alignment between the two groups is optimal, thus enabling the full contribution of the interacting electrical anharmonicity to 2DIR signals.

Although it would be difficult to verify these theoretical predictions experimentally, this preliminary theoretical study clearly showed the structural sensitivity of EVV 2DIR spectroscopy in terms of distances and relative orientations between two interacting groups. This hints at the possibility of developing EVV 2DIR into a structural analysis tool for intermolecular complex formation, in particular the binding of small molecules to proteins, protein−protein interactions, and the interactions of protein side chains within one other protein. In fact, the results with 4-cyano-1-butyne indicate that even for certain intramolecular coupling EVV 2DIR spectroscopy might have some use as a structural analysis tool as long as the coupling is largely electrical.

4. Conclusion

There are now many published examples of several coherent multidimensional spectroscopy techniques using different optical pulse sequences and combinations. These sequences and combinations may be used in different systems depending upon the context of the experiments and the details of implementation. We have sought to illustrate some applications of EVV 2DIR in the biological and biomedical sciences in particular with respect to proteomics and imaging and give a hint of what might be possible in the future for structural analysis of proteins in particular functional states.

BIOGRAPHICAL INFORMATION

Frédéric Fournier obtained his Ph.D. in Physics from University Paris XI-Orsay in 2003. Since 2006, he has been a Postdoctoral Research Associate in the Chemical Biology Centre at Imperial College London, focusing on the development of nonlinear laser spectroscopy methods and their applications to biological problems.

Rui Guo received his Ph.D. in Physical Chemistry in 2000 from Peking University. He is currently a Postdoctoral Research Associate at Imperial College London working on theoretical simulations of EVV 2DIR spectroscopy, in particular the structural−spectral correlation from first-principle calculations.

Elizabeth M. Gardner obtained her M.Res. in Biomolecular Sciences in 2005 from Imperial College London. She is currently completing her Ph.D. with the Chemical Biology Centre based at the same institution. Her research interests include the use of optical spectroscopies for protein analysis, in particular, the development of EVV 2DIR spectroscopy as a protein fingerprinting tool.

Paul M. Donaldson obtained his Ph.D. from Imperial College London in 2008. He is currently a Postdoctoral Research Associate at the University of Zurich working on applying 2DIR methods to the study of energy transport in proteins.

Christian Loeffeld received his M.Sc. from Technical University of Munich and National University of Singapore in 2006. Since 2007, he has been a Ph.D. student at the Chemical Biology Centre at Imperial College London investigating electrokinetic phenomena and applying 2D-IR methods for proteomics-related issues.

Ian R. Gould is a Senior Lecturer in the Department of Chemistry at Imperial College London. His research interests include ab initio chemistry, molecular modeling, molecular dynamics, protein structure−function relationships, sugar and lipid force field development, and nucleic acids.

Keith R. Willison is Professor of Molecular Cell Biology at the Institute of Cancer Research. His research interests include bio-

chemical, kinetic, and structural studies on protein folding, molecular chaperones, and the actin cytoskeleton.

David R. Klug is Professor of Chemical Biophysics in the Department of Chemistry at Imperial College London and Chair of the Chemical Biology Centre. His research interests include natural and artificial solar energy conversion, protein structure−function relationships, and quantitative proteomics and protein networks.

REFERENCES

1 Besemann, D. M.; Condon, N. J.; Murdoch, K. M.; Zhao, W.; Meyer, K. A.; Wright, J. C. Interference, dephasing, and vibrational coupling effects between coherence pathways in doubly vibrationally enhanced nonlinear spectroscopies. *Chem. Phys.* **2001**, *266*, 177–195.

2 Condon, N. J.; Wright, J. C. Doubly vibrationally enhanced four-wave mixing in crotononitrile. *J. Phys. Chem. A* **2005**, *109*, 721–729.

3 Kwak, K.; Cha, S.; Cho, M.; Wright, J. C. Vibrational interactions of acetonitrile: Doubly vibrationally resonant IR-IR-visible four-wave-mixing spectroscopy. *J. Chem. Phys.* **2002**, *117*, 5675–5687.

4 Zhao, W.; Wright, J. C. Measurement of Chi(3) for doubly vibrationally enhanced four wave mixing spectroscopy. *Phys. Rev. Lett.* **1999**, *83*, 1950–1953.

5 Zhao, W.; Wright, J. C. Spectral simplification in vibrational spectroscopy using doubly vibrationally enhanced infrared four wave mixing. *J. Am. Chem. Soc.* **1999**, *121*, 10994–10998.

6 Zhao, W.; Wright, J. C. Doubly vibrationally enhanced four wave mixing: The optical analog to 2D NMR. *Phys. Rev. Lett.* **2000**, *84*, 1411–1414.

7 Donaldson, P. M.; Guo, R.; Fournier, F.; Gardner, E. M.; Barter, L. M. C.; Barnett, C. J.; Gould, I. R.; Klug, D. R. Direct identification and decongestion of Fermi resonances by control of pulse time ordering in two-dimensional IR spectroscopy. *J. Chem. Phys.* **2007**, *127*, 114513.

8 Califano, S. *Vibrational States*; Wiley & Sons: London, New York, Sydney, Toronto, 1976.

9 Donaldson, P. M.; Guo, R.; Fournier, F.; Gardner, E. M.; Gould, I. R.; Klug, D. R. Decongestion of methylene spectra in biological and non-biological systems using picosecond 2DIR spectroscopy measuring election-vibration-vibration coupling. *Chem. Phys.* **2008**, *350*, 201–211.

10 Fournier, F.; Gardner, E. M.; Kedra, D. A.; Donaldson, P. M.; Guo, R.; Butcher, S. A.; Gould, I. R.; Willison, K. R.; Klug, D. R. Proteins identification and quantification by two-dimensional infrared spectroscopy: Implications for an all-optical proteomic platform. *Proc. Natl. Acad. Sci. U.S.A.* **2008**, *105*, 15352–15357.

11 Anderson, N. L.; Anderson, N. G. Proteome and proteomics: New technologies, new concepts and new words. *Electrophoresis* **1998**, *19*, 1853–1861.

12 Blackstock, W. P.; Weir, M. P. Proteomics: Quantitative and physical mapping of cellular proteins. *Trends Biotechnol.* **1999**, *17*, 121–127.

13 James, P. Protein identification in the post-genome era: The rapid rise of proteomics. *Q. Rev. Biophys.* **1997**, *30*, 279–331.

14 Fournier, F.; Gardner, E. M.; Guo, R.; Donaldson, P. M.; Barter, L. M. C.; Palmer, D. J.; Barnett, C. J.; Willison, K. R.; Gould, I. R.; Klug, D. R. Optical fingerprinting of peptides using two-dimensional infrared spectroscopy: Proof of principle. *Anal. Biochem.* **2008**, *374*, 358–365.

15 Flicek, P.; Aken, B. L.; Beal, K.; Ballester, B.; Caccamo, M. Ensembl 2008. *Nucleic Acids Res.* **2008**, *36*, D707–D714.

16 Reilly, R. F.; Ellison, D. H. Mammalian distal tubule: Physiology, pathophysiology and molecular anatomy. *Physiol. Rev.* **2000**, *80*, 277–313.

17 Adachi, S.; Park, S. Y.; Tame, J. R. H.; Shiro, Y.; Shibayama, N. Direct observation of photolysis-induced tertiary structural changes in hemoglobin. *Proc. Natl. Acad. Sci. U.S.A.* **2003**, *100*, 7039–7044.

18 Causgrove, T. P.; Dyer, R. B. Picosecond structural dynamics of myoglobin following photolysis of carbon monoxide. *J. Phys. Chem.* **1996**, *100*, 3273–3277.

19 Denis, M.; Richaud, P. Dynamics of carbon-monoxide recombination to fully reduced cytochrome-c oxidase in plant-mitochondria after low-temperature flash-photolysis. *Biochem. J.* **1982**, *206*, 379–385.

20 Barth, A.; Corrie, J. E. T.; Gradwell, M. J.; Maeda, Y.; Mantele, W.; Meier, T.; Trentham, D. R. Time-resolved infrared spectroscopy of intermediates and products from photolysis of 1-(2-nitrophenyl)ethyl phosphates: Reaction of the 2-nitrosoacetophenone byproduct with thiols. *J. Am. Chem. Soc.* **1997**, *119*, 4149–4159.

21 Rodig, C.; Chizhov, I.; Weidlich, O.; Siebert, F. Time-resolved step-scan Fourier transform infrared spectroscopy reveals differences between early and late M intermediates of bacteriorhodopsin. *Biophys. J.* **1999**, *76*, 2687–2701.

22 McCamant, D. W.; Kukura, P.; Mathies, R. A. Femtosecond stimulated Raman study of excited-state evolution in bacteriorhodopsin. *J. Phys. Chem. B* **2005**, *109*, 10449–10457.

23 Herbst, J.; Heyne, K.; Diller, R. Femtosecond infrared spectroscopy of bacteriorhodopsin chromophore isomerization. *Science* **2002**, *297*, 822–825.

24 Smith, S. O.; Pardoen, J. A.; Lugtenburg, J.; Mathies, R. A. Vibrational analysis of the 13-cis-retinal chromophore in dark-adapted bacteriorhodopsin. *J. Phys. Chem.* **1987**, *91*, 804–819.

25 Scherrer, P.; Mathew, M. K.; Sperling, W.; Stoeckenius, W. Retinal isomer ratio in dark-adapted purple membrane and bacteriorhodopsin monomers. *Biochemistry* **1989**, *28*, 829–834.

26 Bredenbeck, J.; Hamm, P. Peptide structure determination by two-dimensional infrared spectroscopy in the presence of homogeneous and inhomogeneous broadening. *J. Chem. Phys.* **2003**, *119*, 1569–1578.

27 Volkov, V.; Hamm, P. A two-dimensional infrared study of localization, structure and dynamics of a dipeptide in membrane environment. *Biophys. J.* **2004**, *87*, 4213–4225.

28 Wang, J.; Chen, J.; Hochstrasser, R. M. Local structure of β-hairpin isotopomers by FTIR, 2D IR, and ab initio theory. *J. Phys. Chem. B* **2006**, *110*, 7545–7555.

29 Zhuang, W.; Abramavicius, D.; Mukamel, S. Two-dimensional vibrational optical probes for peptides fast folding investigation. *Proc. Natl. Acad. Sci. U.S.A.* **2006**, *103*, 18934–18938.

30 Okumura, K.; Tokmakoff, A.; Tanimura, Y. Structural information from two-dimensional fifth-order Raman spectroscopy. *J. Chem. Phys.* **1999**, *111*, 492–503.

31 Cho, M. Theoretical description of two-dimensional vibrational spectroscopy by infrared-infrared-visible sum frequency generation. *Phys. Rev. A* **2000**, *61*, 023406.

32 Hahn, S.; Kwak, K.; Cho, M. Two-dimensional vibrational spectroscopy. IV. Relationship between through-space vibrational coupling and intermolecular distance. *J. Chem. Phys.* **2000**, *112*, 4553–4556.